

Size Plasmon–Polariton Resonance and Its Contribution to the Giant Enhancement of the Raman Scattering

V. I. Kukushkin^{a, b, *}, Ya. V. Grishina^a, V. V. Solov'ev^a, and I. V. Kukushkin^a

^a *Institute of Solid State Physics, Russian Academy of Sciences, Chernogolovka, Moscow region, 142432 Russia*

^b *Mechnikov Research Institute of Vaccines and Sera, Moscow, 105064 Russia*

*e-mail: kukush@issp.ac.ru

Received April 18, 2017; in final form, April 27, 2017

The dependence of the enhancement of the Raman scattering on the size of a dielectric column is measured in structures with the spatial modulation of the height and lateral sizes of the dielectric coated with a thick metal layer (10–80 nm). It is established that, in the case of a thick metal coating (silver, gold, and copper coatings are used) at dimensions of the dielectric column close to the laser pump wavelength, considerable enhancement of the Raman signal oscillating upon the variation of the geometrical dimensions of the structure is observed. It is shown that the observed resonance enhancement of the Raman signal is associated with the transformation of the electromagnetic radiation into localized plasmon–polariton modes, and the efficiency of such transformation is determined by the commensurability of the wavelength of the plasmon–polariton mode and the planar size of the metal film. For different metal coatings, the dependence of the enhancement of the Raman scattering on the laser wavelength is measured.

DOI: 10.1134/S0021364017100071

The effect of giant enhancement of the Raman scattering found about 40 years ago [1] arises owing to the electron plasma resonance in metal nanoparticles [2–6]. Because of this resonance, the amplitude of the electromagnetic field increases by orders of magnitude, which leads to the giant characteristic enhancement of the Raman scattering of 10^6 – 10^7 [3, 5, 7–9]. It is important that the enhancement of the Raman scattering is not observed on smooth metal surfaces. In this case, scattering is instead suppressed because the dipole moment of a molecule is screened on a smooth metal surface owing to effects of charge imaging in metal [10–13] and, as a consequence, the intensity of the dipole radiation drops. The complete screening of the dipole is impossible on a rough surface, and this problem disappears. In addition, the key point is the probability of transformation of the transverse electromagnetic laser radiation into a longitudinal plasma mode. Surface waves exist on the surface of metals (on the interface of media with positive and negative permittivity) [14–16], i.e., waves running along the surface of the interface, and their amplitude drops exponentially along the normal to the surface on both of its sides. Such waves are called surface plasmons. Surface plasmons do not interact with light waves on a smooth metal surface: they cannot be excited by bulk waves and cannot transfer into them because such transformations cannot satisfy the laws of conservation of energy and momentum simultaneously. Such transformations require, e.g., prisms, diffraction gratings,

or rough surfaces. All these “devices” provide the simultaneous satisfaction of the laws of conservation of energy and momentum. It is important that the energy of surface plasmons is concentrated in a thin layer near the interface with the thickness about the wavelength of the surface plasmon. This means that, if the rough metal surface transfers the pump light wave into surface plasmons, the energy flux density will increase significantly owing to the compression of waves to the surface. As a consequence, the electric field amplitude of the wave increases significantly by a factor of 30–100 according to the estimates in [14–16].

Structures with a thin layer of silver granules [8, 9] on a dielectric, e.g., quartz, substrate are usually used to transform electromagnetic waves into the plasma mode. At the average thickness of the silver layer of less than 5 nm, the size of separated silver granules is 25–35 nm, which provides the transfer of the necessary wave vector on the order of the inverse size of granules during the transformation of the light wave into the plasma wave and back. A significant size spread of silver granules is a certain drawback of such substrates, which complicates the analysis of physical processes occurring at the giant enhancement of the Raman scattering.

In this work, to eliminate this drawback and to detect the spatial (size) resonance of plasmon–polariton waves, we studied regular structures with

smoothly varying geometric parameters. Structures were prepared in the form of dielectric columns (with fixed height and planar sizes) coated with a thick metal layer. The usage of thick metal coatings makes it possible to avoid splitting into granules. We used silver, gold, and copper as the most promising metals.

Periodic dielectric structures were a set of SiO_2 columns with a height of 100–200 nm and planar size a (arranged with the period $2a$), which was varied in the interval of 50–1500 nm. These structures were coated with a metal (silver, gold, or copper) layer with the thickness varied in the interval of 10–80 nm. Such a periodic structure was used for measuring the inelastic light scattering spectrum with the giant enhancement, and as analytes, we applied single-molecular layers of different organic compounds (4-aminobenzotriol, thiophenol, carotene, rhodamine, etc.). It was established that the enhancement of the Raman scattering was almost the same for all used compounds.

No enhancement of the Raman scattering was observed in regions with the smooth metal coating located between the periodically modulated structures, but the luminescence and inelastic light scattering signals were suppressed. The giant enhancement of the Raman scattering was detected in places with the periodic dielectric structures with the thick metal coating, and the enhancement depended on the geometrical parameters of the periodic structure and the laser wavelength. It was shown that the observed resonance enhancement of the Raman signal was associated with the transformation of the electromagnetic radiation into localized plasmon–polariton modes, and the efficiency of such transformation was determined by the commensurability of the wavelength of the plasmon–polariton mode and the planar size of the metal film.

The studied structures were created by the method described in detail in [17]: $100\ 50 \times 50\text{-}\mu\text{m}$ active regions separated by inactive regions with the same size were manufactured on a thermally oxidized silicon substrate (the oxide thickness was 300 nm) (see Fig. 1a taken from [17]). Square columns with the height h and size a arranged with the period $2a$ were made in active regions using electron lithography and plasma etching. Quartz columns were absent in the inactive regions, and these regions served for comparative analysis. The size a of columns in active squares varied in the interval of 50–700 nm with a step of 5 nm. The height of columns was $h = 130$ nm. The entire structure (all active and inactive regions) was coated with a thick metal (silver, gold, or copper) layer with the thickness from 10 to 80 nm using the method of thermal spraying. The spatial Raman intensity distribution on such structures was studied on a Raman microscope, which makes it possible to obtain a spatial resolution to 1 μm , but we chose the size of 10 μm as the optimal diameter of the spot of the focused laser beam (the scan step was also 10 μm). At such size, it is

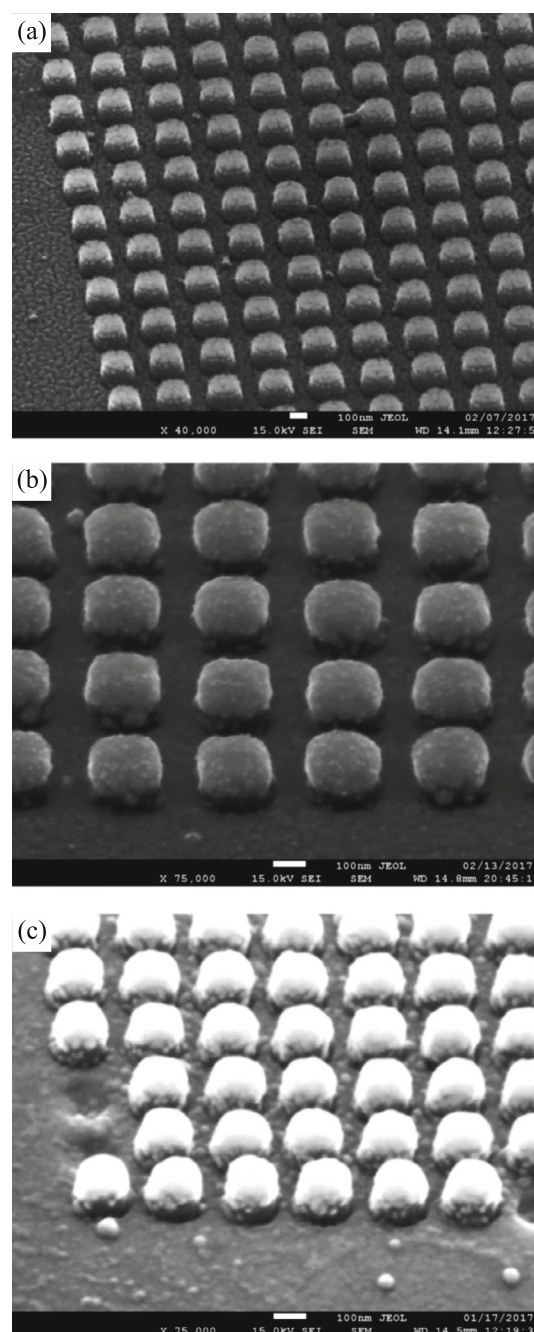


Fig. 1. Photographs of some structures with dielectric columns with (a) 10-nm silver, (b) 40-nm silver, and (c) 40-nm copper coating.

possible to obtain a rather large (for reliable averaging) amount of data on the Raman signal from all active and inactive regions and to scan the whole structure in not too much time. The Raman microscope used in this work allows measurements at several laser wavelengths: 488, 532, and 568 nm. Owing to this circumstance, we studied how the enhancement of the Raman signal depends on the laser wavelength.

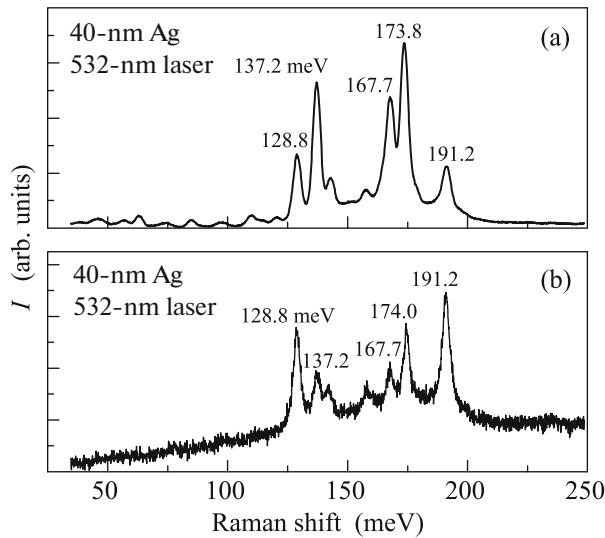


Fig. 2. Raman spectra measured for the 4-aminobenzotriol (4-ABT) organic compound in different active regions of the structures with (a) 40-nm silver and (b) 40-nm gold coating. The laser wavelength is 532 nm.

Figure 1 shows the characteristic photographs of structures obtained on an electron microscope: the columns with the (a) 10-nm silver coating, (b) 40-nm silver coating, and (c) 40-nm copper coating. It follows from the comparison of Figs. 1a and 1b that the granular structure of the metal coating is manifested only in the case of 10-nm silver coating, but completely disappears in the case of 40-nm silver coating, and is absent in the case of gold and copper coatings.

Figure 2 shows Raman spectra with the giant enhancement of the signal measured in optimal regions of the structure with dielectric columns coated with the thick (40 nm) layer of (a) silver and (b) gold. Spectra were recorded for 532-nm laser radiation, and the analyte was the 4-aminobenzotriol (4-ABT) organic compound with the coating in one molecular layer. In the case of silver and gold, the characteristic giant enhancement of the Raman signal of 10^6 (silver) to 10^4 (gold) is observed. It is necessary to note that the same Raman lines are present in the Raman doublet of the silver and gold structures, but the ratios of intensities of separate Raman modes differ dramatically for the silver and gold coatings. In spite of the specified difference in spectra, to determine the giant enhancement for the Raman signal, we measured the integral intensity of all Raman lines in the Raman shift range of 125–200 meV and studied the dependence of the integral signal on the geometrical parameters of the structure, in particular, on the parameter a (the size of the column).

The distribution of the integral intensity of the Raman signal over the surface of the whole structure is shown in Fig. 3 in a pseudocolor representation. It is seen that the Raman intensity in all regions with the

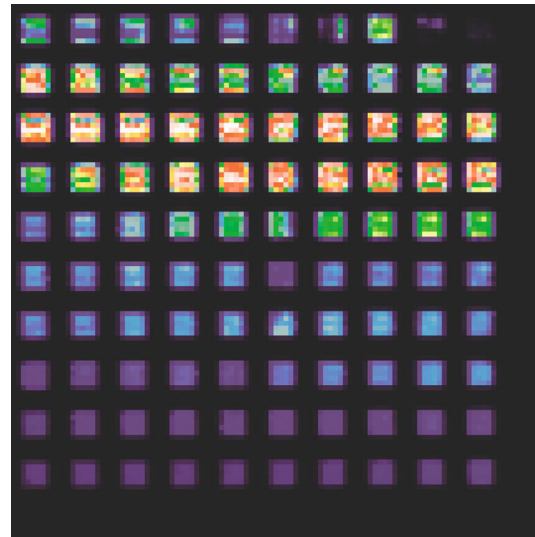


Fig. 3. (Color online) Distribution of the integral intensity of the Raman signal over the surface of the structure consisting of 100 active regions with successively varying geometrical parameters. The spatial resolution of the Raman microscope is 10 μm . The laser wavelength is $\lambda = 532$ nm. The height of dielectric columns is $h = 130$ nm. The organic compound is 4-aminobenzotriol (4-ABT).

spatial modulation of the height and lateral dimensions of the dielectric coated with a thick metal layer significantly exceeds the intensity measured in the regions with a smooth metal coating. Such a distribution was measured on the Raman microscope with a spatial resolution of 10 μm . It also follows from Fig. 3 that oscillations of the integral intensity of the Raman signal are observed at the variation of the parameter a . For the qualitative analysis of the dependences of the Raman intensity on the size a , we calculated the integral intensities of several main Raman lines measured in the center of active regions. For reliability, we averaged the results over nine positions of the laser spot, which with certainty were in the center of these regions.

Figure 4 shows dependences of the integral intensity of the Raman signal on the size a measured on the silver structure with a coating thickness of 40 nm for three wavelengths of the laser excitation. First of all, it is seen that at least two geometrical resonances for all three cases are observed at the positions in the parameter a varying under the variation of the laser wavelength λ . For $\lambda = 488, 532,$ and 568 nm, the main geometrical resonance is observed at $a = 160, 170,$ and 192 nm, respectively. A single-valued relation between the position of the resonance and the laser wavelength, as well as the observation of several resonance maxima, indicates that the origin of the enhancement is in the formation of plasmon–polariton standing waves in the metal layer coating the dielectric column.

The properties of the surface plasmons in thin metal films with close thicknesses of the skin layer and

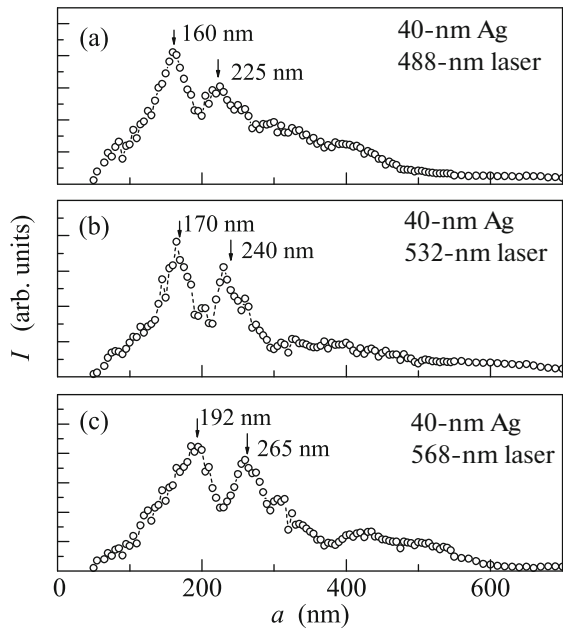


Fig. 4. Integral intensity of the Raman scattering versus the planar size of the quartz column with a height of 130 nm measured at the laser wavelengths of (a) 488, (b) 532, and (c) 568 nm.

film are described in detail in [14–16]. In those works, the dispersion of plasmon–polariton excitations was calculated in these systems with the direct inclusion of the delay effects. In addition, the properties of single thin metal films and multilayer systems consisting of several metal and dielectric layers with different thicknesses were studied in [15]. For the case of a thin metal film sandwiched between dielectrics, two plasmon–polariton modes arise because of the presence of two surfaces of the metal film and the probability of the appearance of in-phase and antiphase oscillations of charges on opposite sides of the film. One of these modes at small wave vectors is described by a linear dispersion law with the velocity $c/\sqrt{\epsilon_d}$, and the frequency of this mode at large wave vectors approaches the asymptotic limit $\omega_p/\sqrt{2}$ from above (ω_p is the plasma frequency of the metal and ϵ_d is the permittivity of the dielectric) [15]. The second mode at small wave vectors is also described by a linear dispersion law, but its effective velocity is somewhat less and depends not only on the permittivity of the dielectric but also on the thickness of the metal film [15]. At large wave vectors, the frequency of the second mode also asymptotically approaches the value $\omega_p/\sqrt{2}$ but from below [15].

We established that the dispersion law of plasmon–polariton waves is satisfactorily described by the formula

$$\omega = ck/\sqrt{\epsilon_{\text{eff}}}, \quad \text{where} \quad \epsilon_{\text{eff}} = (\epsilon_m \epsilon_d)/(\epsilon_m + \epsilon_d). \quad (1)$$

Thus, the geometric resonance condition for different modes of a square plasmon–polariton cavity has the form [14–16]

$$a = \lambda/2\sqrt{(n^2 + m^2)(\epsilon_d + \epsilon_m)/\epsilon_d \times \epsilon_m}, \quad (2)$$

where a is the side of the square, λ is the laser wavelength, $n = 1, 2, \dots$ and $m = 0, 1, 2, \dots$ specify the modes, and ϵ_d and ϵ_m are the permittivities of the dielectric and metal (real part), respectively, depending on the frequency [18]. It follows from Eq. (2) that the ratio of the positions of the first and second resonances is $1/\sqrt{2}$, which is in good agreement with experimental data. The substitution of the permittivities of the metal (silver) and dielectric measured in [18] at the wavelengths of 488, 532, and 568 nm into Eq. (1) gives the following expected wavelengths of resonance modes: 158 and 223 nm (for the laser with $\lambda = 488$ nm), 177 and 250 nm ($\lambda = 532$ nm), and 192 and 272 nm ($\lambda = 568$ nm). These parameters are in very good agreement with those observed in the experiment (see Fig. 4), proving the plasmon–polariton nature of observed geometrical resonances.

To make sure of the occurrence of plasmon–polariton resonance namely in the upper metalized part of columns rather than in the lower part of the structure, we studied samples where the distance between columns was not equal to their size a . As a result, it was established that the position of resonance maxima monitors namely the size of the column rather than the distance between them. This fact unequivocally indicates that the giant enhancement of the Raman scattering occurs on the upper surface of columns coated with a metal.

A separate interesting problem is the dependence of the giant enhancement of the Raman scattering on the thickness of the metal coating. Figure 5 shows these dependences measured on the smooth (nonmodulated) surface and on the structurized region, which were coated with a silver layer with the thickness varying from 2 to 80 nm. The laser wavelength at these measurements was 2 nm. In the case of the smooth surface, the well-known resonance (with an enhancement of about 10^6) is observed at the thickness of silver of about 5–6 nm, which is associated with the formation of a system of silver granules. At the further increase in the thickness of the silver layer, the granular structure disappears, which leads to the sharp decrease in the enhancement and even to the suppression of the Raman signal (at thicknesses larger than 60 nm). The enhancement of the Raman scattering observed in the regions with dielectric columns coated with a metal with the thickness d and optimized geometrical parameters is almost constant, has a weakly expressed maximum at $d = 40$ nm, and is $(1 - 2) \times 10^6$, which is no less than that for the case of silver granules.

It is also of interest to compare how the giant enhancement of the Raman scattering changes in the

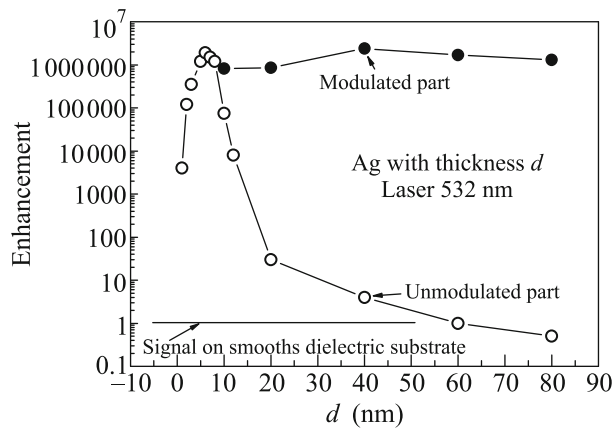


Fig. 5. Enhancement of the giant Raman scattering versus the thickness of the silver coating d measured (open symbols) on the smooth part of the structure and (closed symbols) on the modulated part of the structure with the maximum Raman signal. The laser wavelength is $\lambda = 532$ nm and the column height is $h = 130$ nm. The level of the non-enhanced Raman signal obtained from smooth dielectric (quartz) substrate is also shown for comparison.

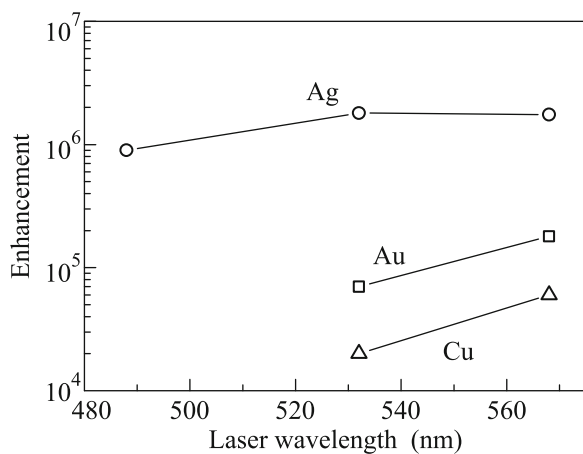


Fig. 6. Giant enhancement of the Raman scattering versus the laser wavelength measured for different metal coatings with the thickness of 40 nm.

case of the thick metal coating with the laser wavelength, and how this depends on the type of metal coating. Figure 6, where the dependences of the enhancement on the laser wavelength measured for the silver, gold, and copper coatings are presented, gives answers to these questions. In the case of short wavelengths ($\lambda < 532$ nm), gold and copper cannot significantly enhance the Raman signal, but the enhancement for these metals increases significantly with the increase in laser wavelength as their permittivities “improve” (the absolute values of the real and imaginary parts increase and decrease, respectively), and at $\lambda > 600$ nm, one should expect approach of the

enhancements for gold and copper coatings to those for silver structures.

To summarize, the dependence of the enhancement of the Raman scattering on the planar size of the metal film has been measured in structures with the spatial modulation of the height and lateral dimensions of the dielectric coated with a 10- to 80-nm-thick metal layer. The resonance enhancement of the giant Raman scattering has been found and attributed to the transformation the electromagnetic radiation into localized plasmon-polariton modes. It has been shown that the efficiency of such transformation is determined by the commensurability of the wavelength of the plasmon-polariton mode and the planar size of the metal film. The dependence of the enhancement of the Raman scattering on the laser pump wavelength is measured for different metal coatings (silver, gold, and copper).

This work was supported by the Russian Science Foundation (project no. 16-15-10332).

REFERENCES

1. M. Fleischmann, P. J. Hendra, and A. J. McQuillan, *Chem. Phys. Lett.* **26**, 163 (1974).
2. M. Moskovits, *Rev. Mod. Phys.* **57**, 783 (1985).
3. K. Kneipp, Y. Wang, H. Kneipp, L. T. Perelman, I. Itzkan, R. R. Dasari, and M. S. Feld, *Phys. Rev. Lett.* **78**, 1667 (1997).
4. A. K. Sarychev and V. M. Shalaev, *Electrodynamics of Metamaterials* (World Scientific, Singapore, 2007).
5. S. Nie and S. R. Emory, *Science* **275**, 1102 (1997).
6. S. A. Lyon and J. M. Worlock, *Phys. Rev. Lett.* **51**, 593 (1983).
7. H. Xu, X. Wang, M. Persson, H. Q. Xu, M. Kall, and P. Johansson, *Phys. Rev. Lett.* **93**, 243002 (2004).
8. V. I. Kukushkin, A. B. Van'kov, and I. V. Kukushkin, *JETP Lett.* **98**, 64 (2013).
9. V. I. Kukushkin, A. B. Van'kov, and I. V. Kukushkin, *JETP Lett.* **98**, 342 (2013).
10. A. Sommerfeld, *Ann. Phys.* **28**, 665 (1909).
11. H. Morawitz, *Phys. Rev.* **187**, 1792 (1969).
12. H. Morawitz and M. R. Philpott, *Phys. Rev. B* **10**, 4863 (1974).
13. G. W. Ford and W. H. Weber, *Phys. Rep.* **113**, 195 (1984).
14. R. H. Ritchie, *Phys. Rev.* **106**, 874 (1957).
15. E. N. Economou, *Phys. Rev.* **182**, 539 (1969).
16. L. Novotny and B. Hecht, *Principles of Nano-Optics* (Cambridge Univ. Press, Cambridge, 2006).
17. V. I. Kukushkin, Ya. V. Grishina, S. V. Egorov, V. V. Solov'ev, and I. V. Kukushkin, *JETP Lett.* **103**, 508 (2016).
18. P. B. Johnson and R. W. Christy, *Phys. Rev. B* **6**, 4370 (1972).

Translated by L. Mosina